Fatigue of hybrid glass/carbon composites: 3D computational studies

CrossMark

Gaoming Dai *, Leon Mishnaevsky Jr. *

Department of Wind Energy, Section of Composites and Materials Mechanics, Technical University of Denmark, Risø Campus, Frederiksborgvej 399, DK-4000 Roskilde, Denmark

ABSTRACT

3D computational simulations of fatigue of hybrid carbon/glass fiber reinforced composites is carried out using X-FEM and multifiber unit cell models. A new software code for the automatic generation of unit cell multifiber models of composites with randomly misaligned fibers of various properties and geometrical parameters is developed. With the use of this program code and the X-FEM method, systematic investigations of the effect of microstructure of hybrid composites (fraction of carbon versus glass fibers, misalignment, and interface strength) and the loading conditions (tensile versus compression cyclic loading effects) on fatigue behavior of the materials are carried out. It was demonstrated that the higher fraction of carbon fibers in hybrid composites is beneficial for the fatigue lifetime of the composites under tension–tension cyclic loading, but might have negative effect on the lifetime under compression-compression, and has mixed effect for the tension–compression cyclic loading. Further, it was observed that while the fiber misalignment has some potential for increasing the fracture toughness of the hybrid composites, it speeds up the fiber damage and leads to the shortening of fatigue life.

© 2014 Elsevier Ltd. All rights reserved.

1. Introduction

High reliability and extended lifetime of wind turbines are the important pre-conditions for the successful development of the renewable energies in Europe. While the traditional fiberglass/polymer composites still remain the most widely used materials for wind turbines, the interest to alternative, stronger, stiffer and lighter composite fibers, first of all, carbon fibers, is growing [1]. However, the lighter, stiffer and stronger carbon fibers have also their weaknesses, first of all, high price (as compared with glass) and relatively low compression strength. That is why hybrid composites containing both glass and carbon fibers attracted an interest of industry and scientists [2,3]. In the best case, it is expected that the hybrid composites could combine the strong sides of glass and carbon fibers, at the same time, compensating for their weakness. According to the analysis of costs and benefits of replacement of glass fibers by carbon fibers for a 8 m blades carried out by Ong and Tsai [4], the full replacement would lead to 80% weight savings, and cost increase by 150%, while a partial (30%) replacement would lead to only 90% cost increase and 50% weight reduction.

The reliability and lifetime of wind turbine blades are determined by the fatigue damage resistance of wind blade materials. In a number of works, the fatigue behavior of hybrid composites has been studied. Shan et al. [5], and Shan and Liao [6] observed that glass–carbon hybrid composites samples demonstrate higher

lifetime both in air and in water compared with all-glass samples, also under static and dynamic fatigue loading. Burks et al. [7] demonstrated in their model that "carbon fiber reinforced composites perform better in fatigue loading, in comparison to glass fiber reinforced composites, due to the fact that the state of stress within the matrix material was considerably lower for carbon fiber reinforced composites eliminating (or at least prolonging) fatigue damage initiation". Wu et al. [8], considering the glass-basalt hybrid composites, noticed that the hybrid effect can reduce the variability of the fatigue life.

Redon [9] studied micromechanisms, and the effects of misalignment and thermal dissipation on the fatigue of hybrid composites, and observed, among others, frictional sliding between carbon and glass fiber bundles in on-axis specimens. For off-axis loading, the main energy dissipation mechanism was the inelastic shear deformation of polymer matrix. The sensitivity of the fatigue lifetime to the fiber misalignment is higher at the higher angle between the fibers and loading. It is of interest that the author observed the localization of heat generation in the composites just prior to the failure. Bach [10] did not observe any positive effect of replacement of 30% glass by carbon fibers in glass fiber reinforced polyesters, either as coupons or in bolted joints, and concluded that there is no benefit in adding carbon fibers (however, the report was published in 1992). In the quite recent studies, Bortolotti [11] tested hybrid, pure glass and pure carbon samples used in used in the spar caps and in the trailing edge reinforcement. From the experiments, it was concluded that the best performance of the composites (longest tensile fatigue lifetime, highest stiff-

* Corresponding authors. Tel.: +45 60697858; fax: +45 46775758 (L. Mishnaevsky).
E-mail addresses: ggda@dtu.dk (G. Dai), lemi@dtu.dk (L. Mishnaevsky Jr.).

ness) is observed in pure carbon fibers for all load ratios; however, there was very large scattering of results for tension–compression loading. At the high compressive loading however, the hybrids led to lowest S–N curves. Summarizing, one can state that the hybrid composites have a high potential for using as highly durable and damage resistant materials in wind turbines. However, their performances depend on a number of microstructural and loading parameters, and these effects should be analyzed both experimentally and theoretically.

In this paper, we seek to analyze the fatigue resistance of hybrid composites and the effects of the hybridization and interaction between different fibers, fiber misalignment and loading conditions on the fatigue behavior. In order to do it, we develop 3D computational unit cell model of hybrid composites with misaligned fibers and carry out systematic numerical simulations of the composite degradation under different loading conditions. In the computational model, we use the effective fiber–matrix interface concept (allowing to take into account the interface degradation and damage) and apply the extended FEM approach. To analyze the effect of microstructural parameters, such as interface material properties, misalignment of fibers, fiber types and distribution in the composites as well as of different loading conditions on the fatigue performance of hybrid fiber reinforced composites.

2. 3D computational model of hybrid fiber reinforced composites (HFRC)

2.1. Automatic generation of 3D models of hybrid misaligned fiber reinforced composites

A special Python based software code has been developed for the automatic generation of 3D multi-element unit cell FE models of hybrid fiber reinforced composites [12]. The program allows varying the fiber orientation (random, aligned, aligned at some angle to the loading direction), radii, arrangements of the fibers. All the fibers are randomly arranged in the matrix, and its location is decided by the two center points on top and bottom face, respectively [13]. The coordinates of the points are generated using the Mersenne Twister random number generator. Each fiber is associated with a misalignment angle, which is also generated using the random number generator. The range of the angle is set to be 0–10°.

In order to model the interface damage, including the non-plane, rough nature of the fiber/matrix interfaces, we used the effective interface concept introduced in [12,14–16]. The material layer surrounding the fiber and taking into account the fiber surface roughness and modified properties of matrix in the close

vicinity of the fibers is represented as a "third material". The interface has layer thickness but quite smaller when compare with the fiber diameter [17].

Fig. 1 shows examples of several unit cells models of hybrid composites: aligned, misaligned, with fibers cut by the cube borders. Here, the so-called "carbon/glass volume ratio" is defined as the ratio of the carbon fiber volume to that of the glass fibers volume in the unit cell.

2.2. Numerical implementation of fatigue analysis

In this model, two stages of fatigue crack growth (onset of crack growth and crack propagation) are considered (see also [18]). A pre-fatigue step is used to introduce initial defects in the model. The model is subjected to a quasi-static loading. Maximum principal stress criterion is involved to govern the initiation of defects [17,19].

Then, the fatigue modeling procedure is activated. The crack propagation is described using the Paris law [20].

The criterion of the onset of fatigue crack is $\frac{N_0}{c_1(\Delta G)^{c_2}} \geqslant 1$. Here, N_0 denotes the number of cycles to the onset, c_1 and c_2 are material constants while ΔG represents the range of strain energy release rate [18].

The fatigue crack growth rate is described by a power law: $\frac{da}{dN} = c_3(\Delta G)^{c_4}$, where da/dN represents the crack growth rate (fatigue crack length growth per loading cycle), c_3 and c_4 are material constants.

The linear elastic fracture mechanics (LEFM) approach and the extended-FEM method [21–24] are employed in the crack propagation analysis. The strain energy release rates are calculated by the Virtual Crack Closure Technique (VCCT) [25–27].

2.3. Fiber and matrix properties

The following properties of matrix, glass and carbon fibers and the effective interface layers of hybrid composites have been used in the simulation [28–33]:

Matrix (Epoxy): Young's modulus of 1.9 GPa, Poisson's ratio of 0.37; tensile strength of 68 MPa, compression strength of 88 MPa.

Carbon fibers: radius 4 μm, Young's modulus of 276 GPa, Poisson's ratio of 0.37; tensile and compressive strengths are 3000 MPa and 2800 MPa, respectively.

Glass fibers: radius 8 μm, Young's modulus is 72 GPa, Poisson's ratio is 0.26; tensile and compressive strengths are 2500 MPa and 1500 MPa, respectively.

The threshold and critical strain energy release rates of different material phases and different fracture modes are as follows
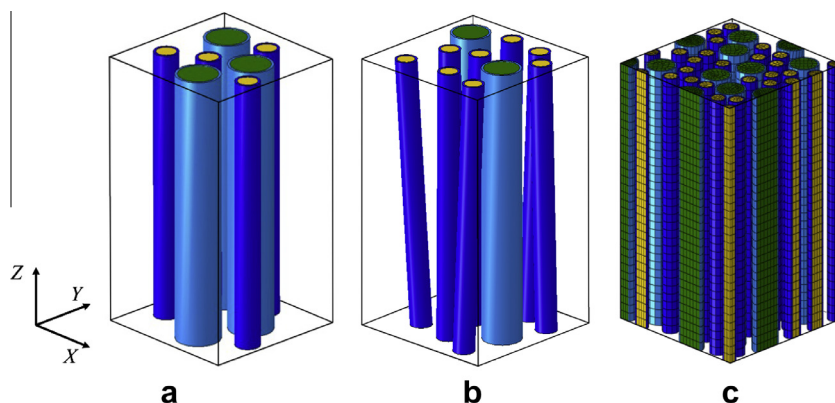
Fig. 1. 3D unit cell models of hybrid composites (a) unidirectional (carbon/glass volume ratio: 1:3), (b) misaligned (carbon/glass volume ratio: 1:1), (c) multi-fiber FE model with fibers cut by the borders.

[34–38]: Matrix: $G_{Ith} = 0.36$ kJ/m^2, $G_{IC} = 0.103$ kJ/m^2, $G_{IIth} = 0.24$ kJ/m^2, $G_{IIC} = 0.648$ kJ/m^2, $G_{IIIth} = 0.306$ kJ/m^2, $G_{IIIC} = 0.850$ kJ/m^2; Glass fiber: $G_{Ith} = 0.21$ kJ/m^2, $G_{IC} = 0.682$ kJ/m^2, $G_{IIth} = 0.651$ kJ/m^2, $G_{IIC} = 2.245$ kJ/m^2, $G_{IIIth} = 0.994$ kJ/m^2, $G_{IIIC} = 2.923$ kJ/m^2; Carbon fibers: $G_{Ith} = 0.919$ kJ/m^2, $G_{IC} = 3.169$ kJ/m^2, $G_{IIth} = 4.995$ kJ/m^2, $G_{IIC} = 12.183$ kJ/m^2, $G_{IIIth} = 4.526$ kJ/m^2, $G_{IIIC} = 16.161$ kJ/m^2; $GM_{Interface}$: $G_{Ith} = 0.058$ kJ/m^2, $G_{IC} = 0.161$ kJ/m^2, $G_{IIth} = 0.738$ kJ/m^2, $G_{IIC} = 2.05$ kJ/m^2, $G_{IIIth} = 0.893$ kJ/m^2, $G_{IIIC} = 2.35$ kJ/m^2; $CM_{Interface}$: 0.144 kJ/m^2, $G_{IC} = 0.379$ kJ/m^2, $G_{IIth} = 0.476$ kJ/m^2, $G_{IIC} = 1.70$ kJ/m^2, $G_{IIIth} = 0.712$ kJ/m^2, $G_{IIIC} = 1.78$ kJ/m^2. Here, $GM_{Interface}$ is the glass–matrix interface while $CM_{Interface}$ stands for the carbon–matrix interface. As a first approximation, we used the four material constants c_1, c_2, c_3 and c_4 from [18]: $c_1 = 2.8461 \times 10^{-9}$, $c_2 = -12.415$, $c_3 = 2.44 \times 10^6$ and $c_4 = 10.61$.

The thickness of this layer was taken as $r/10$, where r stands for the radius of carbon/glass fiber [39]. In so doing, we used also the analysis by Williams et al. [40], who observed that "the modulus data as a function of distance from the fiber surface" and this "distance" is depend on the fiber properties (carbon or glass). When the "distance from the fiber surface" is larger than 1 µm, Young's modulus is practically equal to that of matrix. In our current model, the interface layers surrounding the fibers were assigned average properties between the fibers and matrix. The models were subject to uniaxial static or cyclic loadings along the Z (vertical) direction (uniform on the upper face of the box). The numerical simulations are carried out using the finite element commercial software ABAQUS/STANDARD (version 6.11). The C3D8R element, a 3D 8-node linear brick, reduced integration element, in conjunction with the C3D4, a three-dimensional 4-node linear tetrahedron element, were used in the FE analysis.

3. Computational simulations of fatigue evolution in hybrid composites

In this section, we seek to study the effect of microstructure of composites (fractions of different fibers, misalignment, interface properties) and the loading conditions on the fatigue resistance and lifetime using the computational models described in Section 2.

3.1. Fatigue of hybrid composite: role of fiber mixing

A number of unit cells with different contents of glass and carbon fibers were generated, and subject to tension–tension cyclic loading, displacement controlled, with stress ratio (defined as the ratio of minimum loading to maximum loading) of $R = 0.1$. The unit cell sizes are $42.3 \times 42.3 \times 125$ µm. The total volume content of all fibers was set at 44.9%. Varying the ratio of carbon/glass contents, we vary also the total amount of fibers (given that the radii of glass and carbon fibers differ).

Fig. 2 gives the S–N curves for the unit cells with different carbon/glass content ratios obtained in the simulations. The maximum stresses were normalized by the initial maximum stress of pure carbon fibers reinforced composite, 484.22 MPa.

The S–N curves on Fig. 2 exhibit two regions. The plateau-like region I of high stresses and short lifetimes is apparently controlled by the static damage mechanisms. The part taken by this region increases with increasing the volume fraction of carbon fibers in the hybrid composite. In the region II, controlled by the fatigue degradation of the material, applied stress is quickly reduced with increasing the required lifetime. One can see that the higher the content of glass fibers in the composite and the lower the carbon content, the steeper the reduction of the applied stress as a function of lifetime. The composites with the highest volume fraction of carbon fibers have the highest stress and longest lifetime under
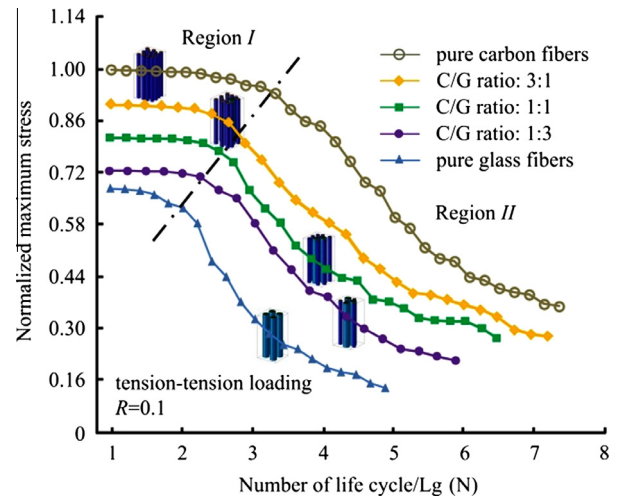
Fig. 2. Comparison of the S–N curves of HFRC with different carbon/glass ratios.

tension–tension (T–T) cyclic loading, while the parameters for the pure glass composites were the lowest.

The pure carbon fiber reinforced composite demonstrate the maximum stress 32.2% higher than those with pure glass reinforcement.

This conclusion confirmed by experiments by Phillips [41]. In his work, the lifetime of composite with 50/50 glass/carbon and pure glass were compared. The stress for the lifetime 106 was 100% times higher for 50/50 composite than for pure glass. In our results, the difference was 85% higher. Thus, our simulations correspond well to these experiments.

The conclusions about the best performances of pure carbon composites and the positive effect of replacement of glass by carbon for cyclic tensile loading is confirmed by the experiments by Bortolotti [11] as well.

Fig. 3 shows the fatigue crack development in a composite with 3:1 carbon/glass ratio. The crack is initiated in a carbon fiber (Fig. 3a), and just after that, other fibers located close to the broken carbon fiber also become damaged (Fig. 3b). At the same time, the crack penetrates into the fiber–matrix interface and then to the matrix. This damage sequence seems to be controlled by the distances between the broken carbon fiber and the intact fibers nearby (Fig. 3c–e). The fibers which are closer to the broken fiber are damaged earlier. Finally, the cracks meet and join together in the matrix. The effect of the distances between fibers on the damage mechanisms and the sequence of damage suggests the possibility to influence the damage resistance of hybrid composites by bundling or clustering of fibers [30].

One can notice that while the damage evolution starts at the carbon fibers (due to their much lower critical strain as compared with that of glass fibers), the higher fraction of carbon fibers still leads to the better S–N curves and longer lifetime of the composite. Apparently, the high stiffness of carbon fibers leads to the higher resistance to the applied stresses. After the damage evolution starts (by failure of a fiber, probably, carbon fiber), the stiffness of the unit cell is reduced, and the strain (at the same stress or force) is reduced as well, the applied strain on the composite becomes lower, thus, reducing the likelihood of further carbon fiber failure.

3.2. Damage growth in interfaces

In order to get a more clear view of the damage evolution in different phases of the composites, we plotted the damage versus loading cycle for fibers, interface and matrix. Fig. 4a shows the

(a) cycle number: 62148	(b) 7.23×10^5	(c) 5.15×10^6	(d) 9.86×10^6	(e) 1.75×10^7
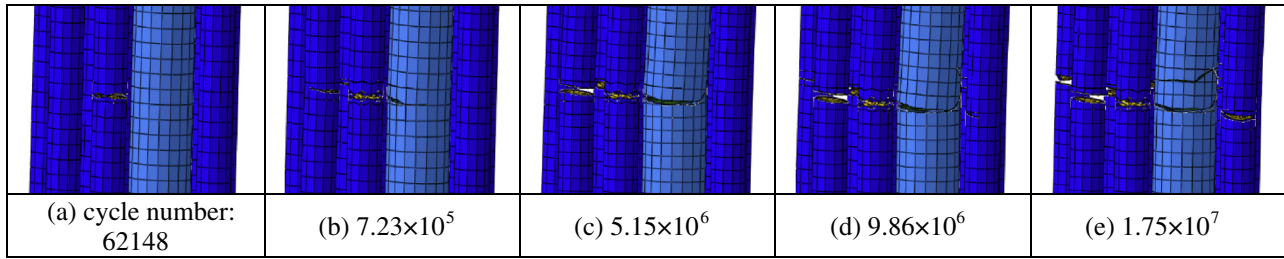
Fig. 3. Crack evolution in a hybrid composite (with carbon/glass volume ratio 3:1).

curves for the hybrid composite with carbon/glass volume ratio of 1:3. The damage parameter is defined as $D = \frac{S_{fail}}{S_{total}}$, where S_{fail} denotes the projection of the crack surface for different material phases on the horizontal X–Y plane, S_{total} is the initial total projected area. For comparison, Fig. 4 presents also the curves for case of the same microstructures, but with two times softer interface (i.e., with Young modulus of one half of the "normal" averaged interface: $E_{W-Inter} = \frac{1}{2}E_{N-Inter} = \frac{1}{4}(E_{Matrix} + E_{Fiber})$. To simplify the comparison, the data on the horizontal axis were all normalized by the cycle-to-failure of interface layer. From the Fig. 4a, one can see that the damage initiates in the carbon fibers, then starts to grow in the interfaces and go over to other neighboring fibers, and later develops in the matrix. This corresponds to the direct observations presented in Section 3.1, Fig. 3.

For the composite with softer interface (i.e., that with lower Young modulus, but the same fracture toughness), the curves for damage in fibers and matrix are similar to those with stiffer interface, but the damage in interface curves are, as expected, different.

In this case, the carbon fibers fail much earlier than in the case with stiffer interfaces. The two times softer interface accelerates the damage of carbon fibers by 54.38%. This is an interesting observation: while the softer interfaces lead to the proportionally shorter lifetimes in matrix, glass fibers and interfaces, its effect on the carbon fibers is much stronger. Apparently, the damage evolution in carbon fibers is very dependent on the interface stiffness.

Fig. 5 shows cross-section views of the damaged hybrid composites with normal and soft interface. In both cases, cracks are formed first in a carbon fiber and then develops into the interface, matrix and in neighboring glass fibers. The main difference is that the crack grows directly into the matrix in the material with stiffer interface (Fig. 5a), and turns into the interface layer if the interface layer is soft (Fig. 5b).

Let us compare the interface damage growth rate under cyclic loading for different structures of hybrid composites. Fig. 6 shows the interface damage parameter as a function of the number of loading cycles, for pure carbon, pure glass composites and hybrid

composites with carbon/glass ratios 1:3, 1:1, 3:1. The horizontal axis is normalized by the lifetime of the interface in pure carbon fiber reinforced composite, 4.27×10^7. One can see that the interface damage growth increases in the following order: pure glass-hybrids 1:3–1:1–3:1 -pure carbon. The interface damage growth rate is highest for the glass and lowest for pure carbon reinforced composites. The interfaces in carbon reinforced composites can sustain 60% more loading cycles than that of glass reinforced composites.

3.3. Fiber misalignment effects in composite fatigue

Here, we study the effect of the fiber misalignment on fatigue behavior of hybrid fiber reinforced composite. We consider the unit cell models with ideally aligned fibers (Fig. 7I) and randomly misaligned fibers (Fig. 7II). In order to exclude all other effects, the volume content (42.3%), carbon/glass ratio (1:1) and fiber arrangements (on the lower horizontal side of the unit cell box) were kept the same in both models.

The misalignment angles of fibers in the 2nd model were randomly varied between 0° and 10°. The models are subjected to tension–tension cycle loading (with stress ratio of $R = 0.1$) along the Z (vertical)-direction.

Fig. 8 shows the normalized S–N curves for the unit cells with aligned and misaligned fiber distribution. The data are normalized by the initial maximum stress of the aligned hybrid FRC composite, 374.43 MPa. One can see that the misalignment clearly reduces the lifetime of composites, especially at the applied loading of the order of 0.3...0.7 of critical maximal stresses, and lower. The lifetime is reduced due to the misalignment by up to 60–65%.

It is of interest to compare this with the results by Mandell and Samborsky [31]. In their experiments, the stress corresponding to 10^6 cycles lifetime decreases due to an addition of 10° misalignment by 17.9%. In our simulations, at the same lifetime, the stress decreases by 22.2%. Given rather rough estimation of input data, it can be said that these experiments confirm our results.
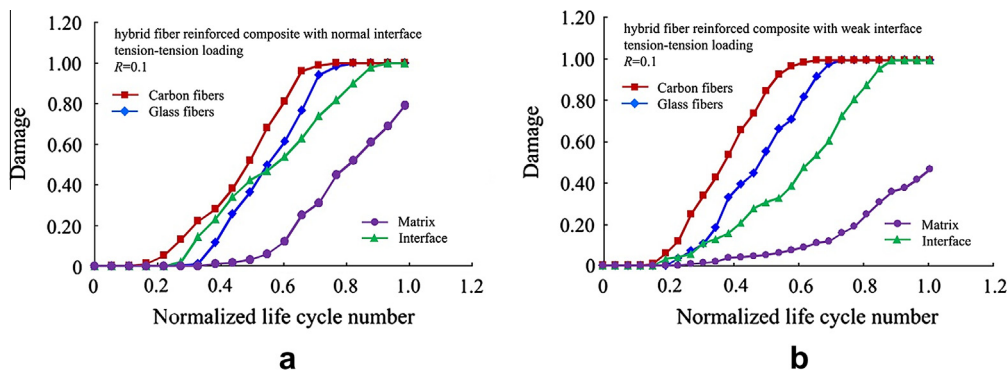
Fig. 4. Damage parameters evolution under tension–tension loading of hybrid FRCs with (a) normal interface (normalized by the cycle number at which the interface is fully damaged, 2.41×10^6), (b) soft interface (similarly, normalized by 1.17×10^6).
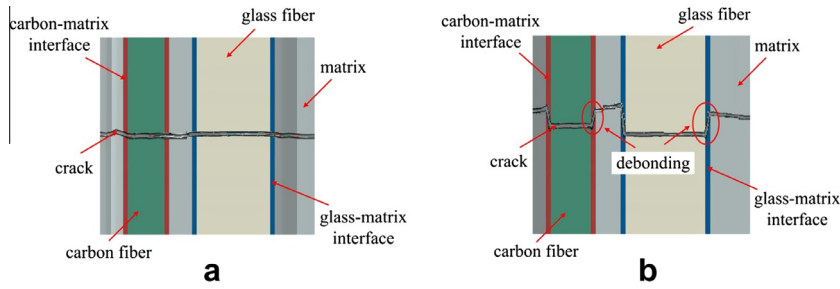
Fig. 5. Micromechanisms of the interface properties effect of hybrid composites (a) normal interface, (b) soft interface.
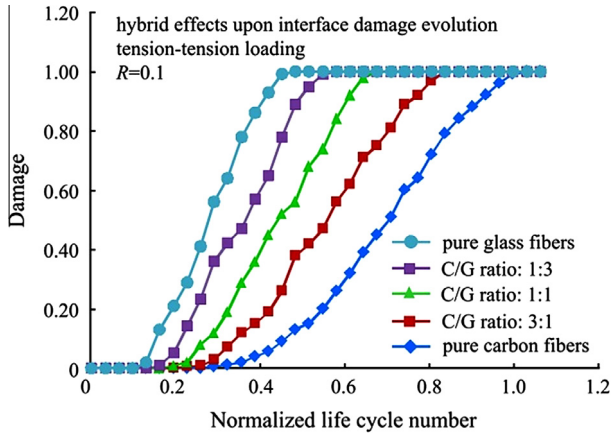
Fig. 6. Interface damage parameter evolution as a function of carbon/glass ratio.

Fig. 8. S–N curves of hybrid composites with aligned and unaligned fibers.

Fig. 9 shows the fatigue crack morphology in aligned and misaligned models, respectively. One can see that the cracks in carbon fibers look differently: while in the aligned composite, the crack surface in carbon fibers is smooth and horizontal (Fig. 9a), one can see the strong crack deviations along the fiber length (probably, shear controlled) in carbon fibers in the misaligned model (Fig. 9b). Thus, one can expect intensive (shear controlled) crack deviations and much more rough fracture surface, as a result of the fiber misalignment in the composites. Redon [9] also observed that the fiber misalignment leads to more energy consuming crack propagation, subject to the strong inelastic shear effects. Still, while the fiber misalignment has some potential for improving the composite performances (e.g., fracture toughness enhancement by crack deviations and fracture surface roughening), it has generally a negative effect of the fatigue lifetime, as noted above and also demonstrated in [30]. Fig. 10 shows the damage parameter evolution for the different material phase for the aligned (Fig. 10a) and misaligned (Fig. 10b) hybrid composites. It can be seen that the carbon fibers are damaged much earlier and the

damage growth goes much more quick in the composites with the random fiber misalignment, than in the composites with aligned fibers. The difference of the damage in carbon fibers in a misaligned and aligned composite is about 25%.

3.4. Effect of compressive cyclic loading on the fatigue lifetime in hybrid composites

Compressive damage mechanisms in composites differ from the tensile damage mechanisms.

One of the main compressive damage mechanisms in hybrid composites can be fiber kinking or buckling [30,42–44]. In this section, we seek to analyze the fatigue behavior of hybrid composites under compression–compression and tension–compression cyclic loading, using the multifiber unit cell models developed above.

3.4.1. Compression–compression loading

A number of unit cells with different carbon/glass ratios were subject to cyclic compression–compression loadings and tested
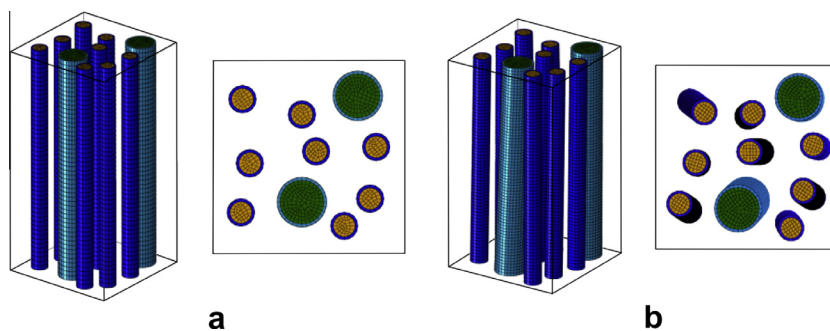
Fig. 7. FEM unit cell models of (a) aligned and (b) misaligned hybrid composites, general and top views.
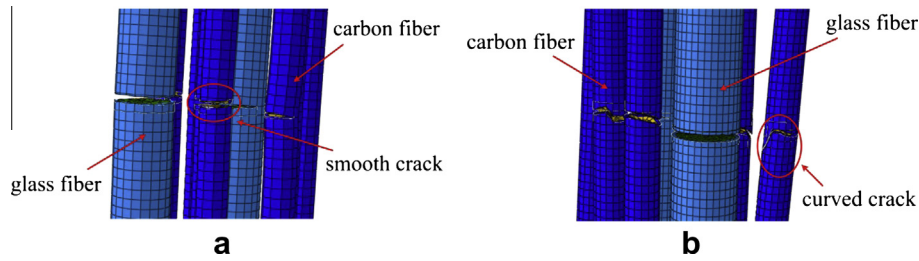
Fig. 9. Crack formation in aligned (a) and misaligned (b) structures.
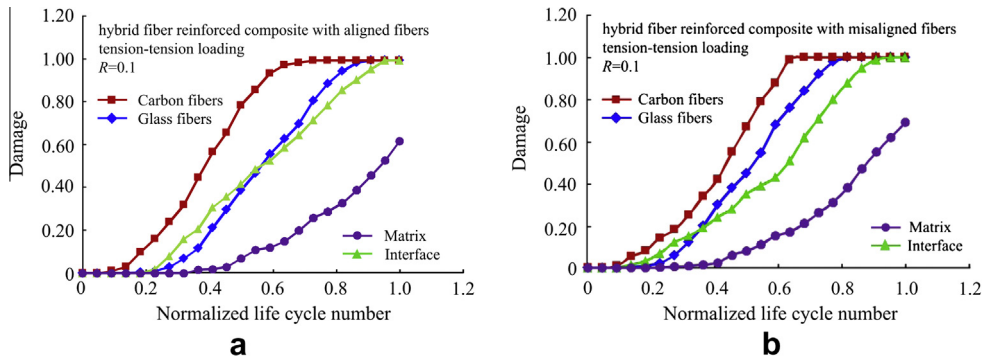
Fig. 10. Damage parameter in main phases plotted versus the life cycle number (a) composite with aligned fibers (normalized by the interface lifetime of 4.16×10^6) (b) composite with misaligned fibers (normalized by the interface lifetime of 3.12×10^6).

in numerical experiments. Assuming the fibers to be elastic and describing the matrix behavior using the Ramberg–Osgood equation, we apply the Budiansky–Fleck model [42] to simulate the compressive damage. Fig. 11 presents the S–N curves of hybrid composites under compression–compression loading.

It is of interest to compare Figs. 13 and 6, obtained for compression–compression (C–C) and tension–tension (T–T) loading, respectively. One can see that the hybrid composites with the highest carbon/glass volume ratio (i.e., largest fraction of carbon fibers) show the lowest maximum stress and fatigue lifetime under C–C cyclic loading. It is the adverse tendency when compared with the T–T loading results shown in Fig. 3.

Fig. 12 shows the fiber damage mechanism observed in simulations. Kinking was found not only in carbon fibers but also in glass fibers. Still, it was observed much more often in carbon fibers. As different from the tension–tension loading, the fiber damage first initiates in glass fibers, and not in carbon. Fibers which are closer to the first damaged glass fiber are damaged next. Fig. 13 shows the damage parameter evolution in different phases of the hybrid composite with carbon/glass volume ratio of 1:1. Again, we can see that carbon fibers get damaged earlier than the glass fibers.

3.4.2. Tension–compression loading

In this subsection, we consider the fatigue behavior of hybrid composites under tension–compression (T–C) cyclic loading, with the stress ratio $R = -1$.

Fig. 14a shows the S–N curves for different hybrid composites under tension–compression loading. One can see that the composite with the carbon/glass volume ratio 3:1 (high carbon content) has the highest maximum stress but the shortest lifetime while the composite with carbon/glass volume ratio 1:3 (low carbon content) has the lowest maximum stress and longest lifetime. We can conclude that the fraction of the carbon fiber in the composites has a strong effect on the fatigue performance of hybrid composites.

The evolution of the damage parameters in different material phases is given in Fig. 14b. The data correspond to a hybrid
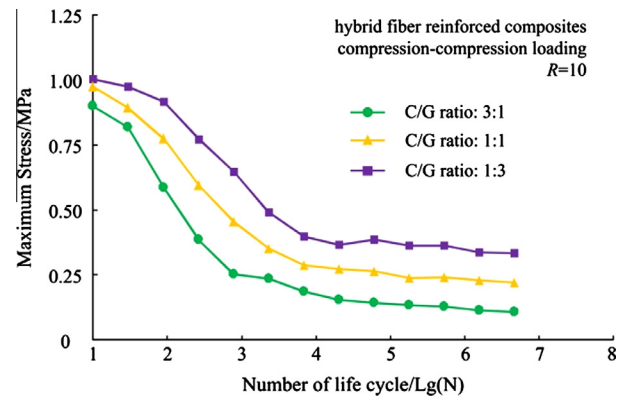
Fig. 11. S–N Curves of different hybrid composites under compression–compression cyclic loading. Vertical axis is normalized by 314.54 Mpa.
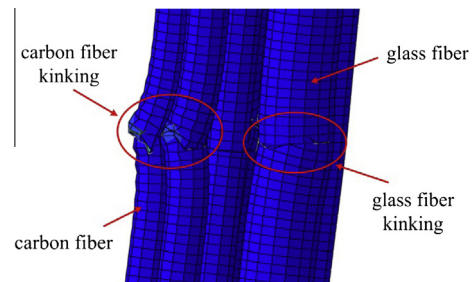
Fig. 12. Kinking of fibers.

composite with 1:1 carbon/glass ratio under T–C cyclic loading. The lifetime is normalized by the maximum interface lifetime, which has the value of 1.43×10^6. One can see, again, that the carbon fibers under T–C cyclic loading start to get damaged earlier and much quicker than the glass fibers. Again, we see that while
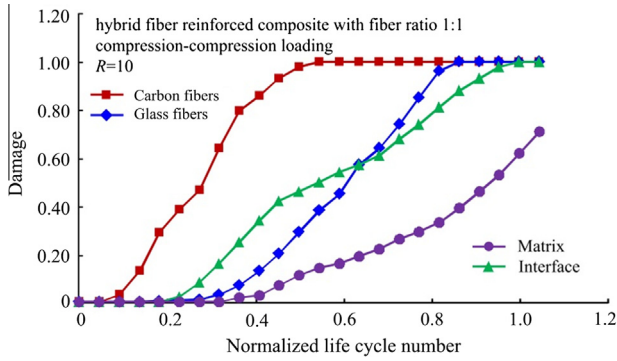
Fig. 13. Damage parameter evolution in 1:1 hybrid composite under compression–compression loading (normalized by the interface lifetime: 3.74 × 106).

the damage evolution in hybrid composites starts at the carbon fibers (both in tensile and compressive loading), but then the higher fraction of carbon fibers in the hybrids ensures the better S–N curves and longer lifetime.

Fig. 15 presents some examples of failure models observed in simulations. It was observed that cracks in glass fibers mainly initiate during the tension period, while cracks on the carbon fibers form during the compression loading period. After a crack is formed in a carbon fiber, it continues to grow during the tension loading period (Fig. 15a) but the failure mode will be changed from mode II (shear fracture, under compression loading) failure to mode I (tensile fracture). Kinking has been observed in both carbon and glass fibers again (Fig. 15b). Thus, our simulation results confirm the damage mechanism of carbon fibers by shear and kinking observed by Hahn [44].

Further, it is of interest to analyze the combined effect of compressive loading and fiber misalignment. Fig. 16a shows the crack formation in a hybrid composite with misaligned fibers. Again, we
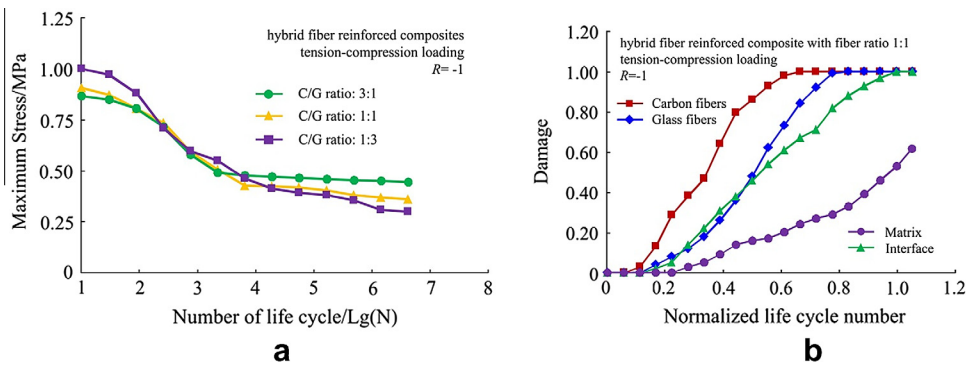
Fig. 14. S–N curve and damage parameter evolution of hybrid FRC under T–C loading (a) S–N curves, (b) damage parameter evolution in 1:1 hybrid FRC. Vertical axis is normalized by 302.21 Mpa.
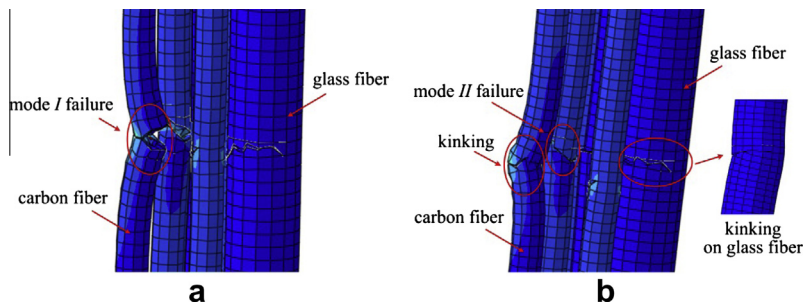
Fig. 15. Different failure modes under tension loading period (a) and compression loading period (b).
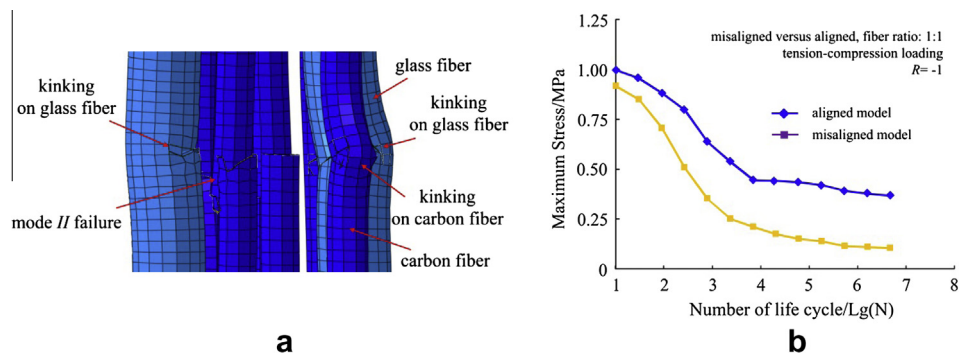
Fig. 16. Observed damage mechanisms in a misaligned hybrid composite under T–C loading (a) and S–N curves (vertical axis is normalized by 256.36 MPa).

see kinking in both carbon and glass fibers. The shear (mode II failure) can be also seen in carbon fiber. Comparing these results with Fig. 15b (unit cell with aligned fibers), we can conclude that the misalignment of fibers increases the crack deflection, and crack surface roughness, and also accelerates the damage growth in fibers. A hybrid composite with high fiber misalignment shows a lower maximum stress and shorter lifetime than that with aligned fibers (see also *S–N* curves, Fig. 16b).

4. Conclusion

Fatigue of hybrid carbon/glass composites is studied using the computational experiments approach, based on 3D multifiber unit cell models and X-FEM.

A Python based software code for the automatic generation of unit cell FE models of hybrid composites with randomly misaligned fibers is developed, and applied in simulations.

Systematic investigations of the effect of microstructure of hybrid composites (fraction of carbon versus glass fibers, fiber misalignment, interface properties) and the loading conditions (tensile and compression cyclic loading) on fatigue behavior of the hybrid composites are presented.

In the computational studies, the following conclusions were made:

- Under tensile–tensile cyclic loadings, composites with the highest volume fraction of carbon fibers show the best performances and longest lifetime, while the parameters for the pure glass composites were the lowest.
- Also under T–T loading, the following damage evolution was observed: a crack is initiated in a carbon fiber, and, in some cases, other microcracks can form in other (carbon or glass) fibers located closely to the broken glass fiber. The fibers which are closer to the failed fiber are damaged. The cracks can propagate into fiber/matrix interface (if the interface is weak), or can grow straight into the matrix. Finally, the cracks join together in the matrix.
- The fiber misalignment has some potential for increasing the fracture toughness of the hybrid composites, since the intensive (shear controlled) crack deviations and much more rough fracture surface can be expected as a result of the fiber misalignment in the composites. Yet, the fiber misalignment speeds up the fiber damage and clearly reduces the lifetime of composites. Carbon fibers are damaged much earlier and the damage growth goes much more quick in the composites with the random fiber misalignment, than in the composites with aligned fibers.
- The stiffness of fiber/matrix interface has a strong effect on the lifetime of composites, especially on the strength and damage of carbon fibers.
- Under compression–compression loading, hybrid composites with the highest carbon/glass volume ratio (i.e., largest fraction of carbon fibers) show the lowest maximum stress and fatigue lifetime. In this case, the fiber damage initiates in carbon fibers. Under tension–compression cyclic loading, after a crack is formed in a carbon fiber, it continues to grow during the tension loading period but the failure mode will be changed from mode II (shear fracture, under compression loading) failure to mode I (tensile fracture).

Acknowledgements

References

[1] Mishnaevsky Jr L, Brøndsted P, Nijssen R, Lekou DJ, Philippidis TP. Materials of large wind turbine blades: recent results in testing and modelling. Wind Energy 2012;15:83–97.

[2] Summerscales J, Short D. Carbon fiber and glass fiber hybrid reinforced plastics. Composites 1978:157–66.

[3] Mishnaevsky Jr L. Composite materials for wind energy applications: micromechanical modelling and future directions. Computat Mechan 2012;50:195–207.

[4] Ong CH, Tsai SW. The use of carbon fibers in wind turbine blade design: A SERI-8 Blade Example SAND2000-0478, Sandia National Laboratories Contractor Report; 2000.

[5] Shan Y, Lai KL, Wan KT, Liao K. Static and dynamic fatigue of glass–carbon hybrid composites in fluid environment. J Compos Mater 2002;36:159–72.

[6] Shan Y, Liao K. Environmental fatigue of unidirectional glass–carbon fiber reinforced hybrid composite. Compos Part B: Eng 2001;32:355–63.

[7] Burks B, Middleton J, Kumosa M. Micromechanics modeling of fatigue failure mechanisms in a hybrid polymer matrix composite. Compos Sci Technol 2012;72:1863–8.

[8] Wu ZS, Wang X, Iwashita K, Sasaki T, Hamaguchi Y. Tensile fatigue behaviour of FRP and hybrid FRP sheets. Compos Part B 2010;41:396–402.

[9] Redon O. Fatigue damage development and failure in unidirectional and angle-ply glass fibre/carbon fibre hybrid laminates. Risø, Report 2000; Risø-R-1168 (EN).

[10] Bach PW. Fatigue properties of glass- and glass/carbon-polyester composites for wind turbines. Netherlands Energy Research Foundation, Report 1992; ecn-c–92-o72.

[11] Bortolotti P. Carbon glass hybrid materials for wind turbine rotor blades. Master Thesis Delft University of Technology; 2012.

[12] Mishnaevsky Jr L, Brøndsted P. Three-dimensional numerical modelling of damage initiation in UD fiber-reinforced composites with ductile matrix. Mater Sci Eng: A 2008;498:81–6.

[13] Mishnaevsky Jr L. Functionally gradient metal matrix composites: numerical analysis of the microstructure–strength relationships. Compos Sci Technol 2006;66:1873–87.

[14] Wang HW, Zhou HW, Mishnaevsky Jr L, Brøndsted P, Wang LN. Single fibre and multifibre unit cell analysis of strength and cracking of unidirectional composites. Computational Materials Science 2009;46:810–20.

[15] Wang HW, Zhou HW, Peng RD, Mishnaevsky Jr L. Nanoreinforced polymer composites: 3D FEM modeling with effective interface concept. Compos Sci Technol 2011;71:980–8.

[16] Peng RD, Zhou HW, Wang HW, Mishnaevsky Jr Leon. Modeling of nano-reinforced polymer composites: Microstructure effect on Young's modulus. Computational Materials Science 2012;60:19–31.

[17] Bunsell AR, Harris B. Hybrid carbon and glass fiber composites. Composites 1974;5:157–64.

[18] Dai GM, Mishnaevsky Jr L. Damage evolution in nanoclay-reinforced polymers: a three-dimensional computational study. Compos Sci Technol 2013;74:67–77.

[19] Dai GM, Mishnaevsky Jr L. Fatigue of multiscale composites with secondary nanoplatelet reinforcement: 3D computational analysis. Compos Sci Technol 2014;91:71–81.

[20] Krueger R. Development of a benchmark example for delamination fatigue growth prediction. Proc-Am Soc Compos 2010;2(Conf 25):948–67.

[21] Belytschko T, Gracie R, Ventura G. A review of extended/generalized finite element methods for material modeling. Modell Simul Mater Sci Eng 2009;17:1–24.

[22] Belytschko T, Black T. Elastic crack growth in finite elements with minimal remeshing. Int J Numer Meth Eng 1999;45:601–20.

[23] Stolarska M, Chopp DL, Moes N, Belyschko T. Modelling crack growth by level sets in the extended finite element method. Int J Numer Meth Eng 2001;51:943–60.

[24] Sukumar N, Moes N, Moran B, Belytschko T. Extended finite element method for three-dimensional crack modeling. Int J Numer Meth Eng 2000;48:1549–70.

[25] Rybicki EF, Kanninen MF. A finite element calculation of stress intensity factors by a modified crack closure integral. Eng Fract Mech 1977;9:931–8.

[26] Mishnaevsky Jr L, Lippmann N, Schmauder S. Computational modeling of crack propagation in real microstructures of steels and virtual testing of materials. Int J Fracture 2003;120:581–600.

[27] Krueger R. Virtual crack closure technique: history, approach and applications. Appl Mech Rev 2004;57:109–43.

[28] Mishnaevsky Jr L, Brøndsted P. Micromechanical modeling of damage and fracture of unidirectional fiber reinforced composites: a review. Comput Mater Sci 2009;44:1351–9.

[29] Mishnaevsky Jr L, Dai GM. Hybrid carbon/glass fiber composites: Micromechanical analysis of structure–damage resistance relationships. Comput Mate Sci 2014;81:630–40.

[30] Mishnaevsky Jr L, Brøndsted P. Statistical modelling of compression and fatigue damage of unidirectional fiber reinforced composites. Compos Sci Technol 2009;69:477–84.

[31] Mandell JF, Samborsky. DOE/MSU Composite Material Fatigue Database: Test Methods, Materials, and Analysis. Report SAND97-3002, Sandia, Albuquerque (NM); 1997.

[32] Qing H, Mishnaevsky Jr L. Unidirectional high fiber content composites: automatic 3D FE model generation and damage simulation. Comput Mater Sci 2009;47:548–55.

[33] Mishnaevsky Jr L, Lippmann N, Schmauder S. Computational modeling of crack propagation in real microstructures of steels and virtual testing of artificially designed materials. Int J Fracture 2003;120:581–600.

[34] Reeder JR. 3D Mixed-mode delamination fracture criteria-an experimentalist's perspective. NASA Langley Research Center, M/S 188E, Hampton VA 23681–2199, USA.

[35] Liao WC, Sun CT. The determination of mode III fracture toughness in thick composite laminates. Comp Sci & Tech 1996;56(4):489–99.

[36] Reeder JR. A bilinear failure criterion for mixed-mode delamination. In: Camponeschi, Jr., editor. Composite Materials: Testing and design, ASTM STP 1206. W. Conshohochen (PA): ASTM Int.; p. 303–22.

[37] Pinho ST, Robinson P, Iannucci L. Fracture toughness of the tensile and compressive fiber failure modes in laminated composites. Compos Sci Technol 2006;66:2069–79.

[38] Jose S, Kuma RK, Jana MK, Rao GV. Intralaminar fracture toughness of cross-ply laminate and its constituent sub-laminates. Compos Sci Technol 2001;61:1115–22.

[39] Siddiqui NA, Sham ML, Tang BZ, Munir A, Kim JK. Tensile strength of glass fibers with carbon nanotube-epoxy nanocomposites coating. Compos: Part A 2009;40:1606–14.

[40] Williams JG et al. Properties of the interphase in organic matrix composites. Mater Sci Eng: A 1990;126(1–2):305–12.

[41] Phillips LN. The hybrid effect-does it exist? Composites 1976;7:7–8.

[42] Budiansky B, Fleck NA. Compressive failure of fiber composites. J Mech Phys Solids 1993;41:183–211.

[43] Zhou HW, Yi HY, Gui LL, Dai GM, Peng RD, Wang HW. Leon Mishnaevsky Jr., Compressive damage mechanism of GFRP composites under off-axis loading: Experimental and numerical investigations. Composites Part B: Engineering 2013;55:119–27.

[44] Hahn HT, Williams JG. Compression failure mechanisms in unidirectional composites. Composite Materials: Testing and Design, ASTM STP 893, Whitney JM, editor, Philadelphia; 1986. p. 115–39.